Journal Pre-proof

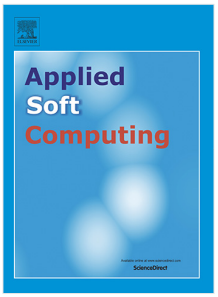

An evolutionary intelligent control system for a flexible joints robot

Alejandro Pena, Juan C. Tejada, Juan David Gonzalez-Ruiz, Lina María Sepúlveda-Cano, Francisco Chiclana, Fabio Caraffini, Mario A. Gongora

PII: S1568-4946(23)00061-3
DOI: https://doi.org/10.1016/j.asoc.2023.110043
Reference: ASOC 110043

To appear in: *Applied Soft Computing*

Received date : 10 October 2022
Revised date : 26 December 2022
Accepted date : 22 January 2023

Please cite this article as: A. Pena, J.C. Tejada, J.D. Gonzalez-Ruiz et al., An evolutionary intelligent control system for a flexible joints robot, *Applied Soft Computing* (2023), doi: https://doi.org/10.1016/j.asoc.2023.110043.

An Evolutionary Intelligent Control System for a Flexible Joints Robot

Alejandro Pena[a], Juan C. Tejada[b], Juan David Gonzalez-Ruiz[c], Lina María Sepúlveda-Cano[a], Francisco Chiclana[d], Fabio Caraffini[e], Mario A. Gongora[d]

[a]*Grupo de Investigación en Información y Gestión, Universidad EAFIT, Carrera 49 # Calle 7 Sur - 50, Medellín, 050022, Antioquia, Colombia*
[b]*Computational Intelligence and Automation Research Group, Universidad EIA, Calle 25 Sur # 42 - 73, Envigado, 055413, Antioquia, Colombia*
[c]*Departamento de Economía, Grupo de Investigación en Finanzas y Sostenibilidad, Universidad Nacional de Colombia, Carrera 65# 59a - 416, Medellín, 050034, Antioquia, Colombia*
[d]*Institute for Artificial Intelligence (IAI), De Montfort University, Gateway House, Leicester LE1 9BH, Leicester, LE19BH, United Kingdom*
[e]*Swansea University, Swansea SA2 8PP Wales, Wales, SA28PP, United Kingdom*

Abstract

In this paper, we present a model for a serial robotic system with flexible joints (RFJ) using Euler-Lagrange equations, which integrates the oscillatory dynamics generated by the flexible joints at specific operating points, using a pseudo-Ornstein-Uhlembeck process with reversion to the mean. We also propose a Stochastic Flexible - Adaptive Neural Integrated System (SF-ANFIS) to identify and control the RFJ with two degrees of freedom. For the configuration of the model, we use two adaptive strategies. One strategy is based on the Generalised Delta Rule (GDR). In contrast, a second strategy is based on the EDA-MAGO algorithm (Estimation Distribution Algorithms - Multi-dynamics Algorithm for Global Optimisation), improving online learning. We considered three stages for analysing and validating the proposed SF-ANFIS model: a first identification stage, a second stage defined by the adaptive control process, and a final stage or cancellation of oscillations. Results show that, for the identification stage, the SF-ANFIS model showed better statistical indices than the MADALINE model in control for the second joint, which presents the greatest oscillations; among those that stand out, the IOA (0.9955), VG (1.0012) and UAPC2 (-0.0003). For the control stage, The SF-ANFIS model showed, in a general way, the best

behaviour in the system's control for both joints, thanks to the capacity to identify and cancel oscillations based on the advanced sampling that defines the EDA algorithm. For the cancellation of the oscillations stage, the SF-ANFIS achieved the best behaviour, followed by the MADALINE model, where it is highlighted the UAPC2 (0.9525) value.

Keywords: Adaptive Neural Fuzzy Integrated Systems (ANFIS), Stochastic Model, System Control, Robotics, Ornstein–Uhlenbeck (OU)

1. Introduction

Robots and humans have increased their interaction more than ever in the last few decades. It is indeed common to have shared spaces where this interaction takes place for multiple purposes and goals, these being, e.g., the use of robotic tools in precision surgery [1, 2], intelligent transportation [3, 4], cognitive sciences [5, 6], ambient assisted living [7, 8], etc., and for this reason precaution measures must be taken to minimise the risk of physical contacts [9, 10]. A great deal of research is currently undertaken to facilitate human-robot interaction, and communication [11, 12] to avoid the risk of misinterpreting a command and involuntarily causing damage. However, even more attention is being paid to the hardware side, and specific materials are employed to produce the so-called Robots with Flexible Joints (RFJ), often integrating also passive protections in their links to minimise collision damages [10].

The classic approach of using mathematical, phenomenological or semi-physical models based on forces, inertias, and energies [13, 14] is successful when the kinematics of the robots are simple but are currently being overcome by more modern approaches that can be efficiently used to describe complex systems without having the burden of checking applicability hypotheses of existing mathematical models of designing new ones. Several examples of this can be found in the scientific literature. In [15] an optimisation algorithm is used to train a neural system to approximate the kinematic model of robotic arms, while a recurrent fuzzy wavelet neural network is employed in [16] for controlling industrial robot manipulators. However, RFJs are often characterised by multiple disturbs jeopardising their stability and operational accuracy [17, 18]. These cannot be easily eliminated with off-the-shelf methods and require combining multiple Computational Intelligence (CI) tools to remove and provide robust control.

The remainder of the paper is organised as follows: in Section 2 and 3, we review the literature that discusses the theoretical foundations for modelling complex systems. In Section 4, we explain the experimental results achieved by the proposed model. We analyse the results in Section 5. Finally, in Section 6, we present a series of conclusions and recommendations to continue developing this research.

2. Literature review

The presence of oscillatory disturbs in RFJs makes it challenging to stabilise these robotic systems, mainly due to the stochastic nature of these undesired inputs. For this reason, apart from specific cases, e.g. [19], classic deterministic approaches often fail at minimising their disruptive effects, and self-adaptive heuristic models are therefore being investigated. Given the success obtained by employing CI paradigms to fine-tune [20], optimization models [21], minimise disturbances [22] and control the dynamics of robotic structures [23, 24], in the last decade researchers have explored various CI-based methods also for dealing with RFJs. That is the case of [25], where the authors use two Neural Networks (NN) to identify the dynamic system, one each for the "fast" (active response) and one for the "slow" (passive response) phenomena.

In this sense, some approaches attempt to improve the learning process in neural models used to identify and control complex systems with stochastic behaviours [26, 27].

Three works, in particular, show the different adaptive processes to improve models' learning with fuzzy neural structures. The first one is an approach that includes Estimation Distribution Algorithms (EDA) as a main stochastic algorithm to optimise the learning in the identification of stochastic systems [28, 29], an Adaptive Neural Fuzzy Integrated Systems model, that use a Particle Swarm Optimisation (PSO-ANFIS) to design dynamical Adaptive Neural Fuzzy Integrated System (ANFIS) structures for identification and modelling complex systems [30, 31], and to identify complex stochastic systems using large ordered linear neural networks, maintaining the balance between accuracy and low computational cost [32]. The second approach is an algorithm that allows optimising the membership functions and fuzzy rules in a canonical ANFIS model as presented in [33]. The last method, shown in [34], established a novel methodology to model random perturbations in wind power plants using an Orstein Ouhnlembeck stochas-

tic model. These works focused on modelling the stochastic process using ANFIS structures supported by different learning methods and techniques, improving the stability in controlling dynamic systems with stochastic behaviours.

Other approaches look at the stability and control of complex stochastic systems, both with NN and with Fuzzy Systems as in [35, 36] respectively. Accordingly, [37] presents an adaptive neural controller for complex systems with unknown stochastic disturbances, where the system's stability was achieved using a *state-feedback* controller based on a Lyapunov function. Dynamic Fuzzy Stochastic Neural Network models for non-parametric identification using vibration data can overcome the limitations imposed by the imprecision in the sensed data using fuzzy concepts as in [38, 39]. In [40] the authors aim to tackle the neural robust tracking control problem for a class of nonlinear systems using an adaptive critic technique. The main contribution is an NN-based tracking control scheme integrating matched uncertainties. Another study developed a Self-Evolving Function-Link Interval Type-2 Fuzzy Neural Network (SEFT2FNN), where the rules and membership functions were obtained autonomously following the behaviour of a complex system [41].

Following on the fuzzy sets in a SEFT2FNN model, [42] presents a robust adaptive control for nonlinear systems using non-triangular fuzzy sets, where the behaviour of the system and their stochastic disturbances are unknown. The results show the convergence of the model towards minor probability errors. Relating the stability of Stochastic Fuzzy Neural Networks with parameter uncertainties, [43] proposes a new mean square exponential stability condition in a control process. Looking at these recent publications, the use of different Adaptive Fuzzy Neural models to improve the stability in complex systems with stochastic behaviour becomes apparent. The common element includes fuzzy systems enabling the use of linguistic variables in the control of complex processes.

Regarding this research, we propose a Stochastic Flexible Neural Fuzzy Integrated System (SF-ANFIS) to identify and control an experimental serial RFJ with two degrees of freedom with brand Quanser as shown in Figure 1. We model the serial RFJ system using Euler Lagrange equations, integrating the oscillatory dynamics generated by the flexible joints in particular operational points (e.g. where a change of direction occurs or at the stopping points [44]). The effect of the oscillatory dynamics was modelled using a sinusoidal signal, configuring a novel methodology to model complex coupled

systems with stochastic behaviours. To identify the serial RFJ, we use two flexible versions of an ANFIS model, integrating an Ornstein Ouhlembeck (OU) stochastic process with mean reversion to cancel the disturbances or the oscillatory dynamics setting the SF-ANFIS model.

One SF-ANFIS version is created using Generalized Delta Rule (GDR) learning. In this stage, the model was evaluated using two neural models: a Multi Adaptive Linear (MADALINE) model [45] and a Fuzzy Stochastic Neural model [39].

We evaluated our proposal using the SF-ANFIS model mentioned above, including a controller based on a Self Tuning PID structure as proposed by [46]. The SF-ANFIS model achieved the best results in the identification and control stages. It resulted in a lower persistence of the disturbances around the SetPoint in specific operational points in the control process. In this way, the stability in the control process was achieved by the ability of the model to cancel disturbances using an integrated OU process, configuring an integrated novel model to control complex coupled systems with stochastic behaviour, as inherent in Serial RFJ systems.

3. Framework for Identification and Control of RFJs

Control of RFJs has gotten attention due to their complexity and real-world application. In general, the RFJs include harmonic drivers to reduce velocity, but it induces torsional elasticity with complex oscillations on the robot joints [47]. For this reason, this paper covers two significant areas of knowledge: one topic focused on typical identification procedures for complex systems and a second focused on the control of stochastic systems that defines the dynamics of RFJs.

3.1. Typical Identification Procedures

In this field of knowledge, two strategies, in general, are used to perform the identification of dynamic systems.

A first strategy, or offline estimation, is based on controlled tests where the system is excited with specific signals, and the outputs are measured. In [48], for example, these offline strategies are used to perform the identification of dynamic systems based on grey-box models and phenomenological principles, which makes them ideal for the design of controllers with fixed structures due to the low variation of the parameters in terms of the time.

The second strategy, or online identification, is where the parameters of the mathematical models are adjusted so that the behaviours become more accurate in representing a real system, which is usually used to perform adaptive control tasks as well by estimating parameters. In the literature, different studies support this strategy; for example, in [49] the authors propose the design and testing of disturbance observers to identify online constants of the springs in a coupled-masses system for applications in flexible joint manipulators. The main complexity in the dynamics of these manipulators' topology is the passive behaviours and the accumulation of energy as a function of joint position variation.

Therefore, it is necessary to identify closed-loop dynamics to ensure that the robot has an optimal reference input to execute the identification procedure correctly. A second paper shows the use of Weighted Least Squares (WLS) and Maximum-Likelihood (ML) techniques to estimate the values for the parameters that define robot dynamics; as well as the noise variance estimation to obtain a suitable weight matrix for the WLS estimator [50]. A final paper shows the identification of parameters online for robots using PID decentralised controllers to generate the control inputs, which further reinforces the importance of online identification methods for complex systems [51].

3.2. Control Strategies for Flexible Joint Manipulators

Conventional control methods are generally insufficient to adapt to time variations of the parameters in RFJs [52]. However, it must also be clear that the adaptive control structures depend on the identification process, which carries a high computational load. In this way, [9] presented a historical comparison of control systems used in RFJs since the 80's. This paper shows that one of the significant challenges in controlling flexible joints is the variability of the functions for different trajectories and payloads of the end effector. Control structures that fix function parameters have been proposed to tackle this problem. One of the control techniques commonly used is feedback linearisation based on Linear-Quadratic Regulator (LQR) controllers. It is even implemented into educational platforms, as in the case of the two Degrees of Freedom (DoF) serial flexible joint robot manipulators developed by Quanser [53] (Figure 1). Among the fixed control structures, we can consider works such as the one developed by [54], which focuses on experimental offline identification to apply computed torque techniques and minimisation of the effects of Friction Compensating Torque (FCT).

Figure 1: Quanser Robot with two Degrees of Freedom (DoT)

The problem of fixed control structures lies precisely in considering the potential variations of flexible robot dynamics regarding load variations or trajectories, specifically in systems with non-linear behaviours. [55] shows the use of adaptive controllers based on decoupled structures for optimal control, among which the LQR controllers also stand out, where the main goal is to tune the gains of the controller to adapt it in terms of different payloads attached to the manipulator. This study attempt to solve the problem of direct adaptive control for endpoint trajectory tracking for a lightweight robot under various loads with minimum computational effort. As in the previous section, the development of controllers that adapt to the behaviour of systems based on the inertia of dynamic systems is an important problem for RFJs control, which reinforces the concept of online identification and control

4. Methodology

One of the most important issues in identifying and controlling complex systems, such as RFJs, is the coexistence of coupled dynamics with stochastic responses and configuring these systems as Stochastic Robots with Flexible Joints (SRFJs). These systems require general adaptive models with flexible structures to better understand their behaviour. For this reason, we present an SF-ANFIS model for online identification and control of SRFJs (Figure 1), for which the following methodology is proposed.

4.1. Experimental Setup

For the development and evaluation of the proposed SF-ANFIS model, an RFJs from the Quanser series was selected as a case study (Figure 1). In the first stage of the experimental study design, we proceed with the modelling of the system using the Euler-Lagrange equations and the Simulink® platform (Figure 2), considering two integrated dynamics: a first dynamic (active dynamic) which describes the general behaviour of the joints that make up an RFJs ($1 - joint$, $2 - joint$); and a second dynamic, which represents the behaviour of the joints in Operating Point where the system Changes of Direction (OPCDs).

In a second stage of the experimental study design, we identified the SRFJs system using the proposed SF-ANFIS model. For the configuration of the model, we use two adaptive strategies. One strategy is based on the Generalised Delta Rule (GDR), while a second strategy is based on the EDA-MAGO algorithm [28]. Two adaptive identification models were used to evaluate the SF-ANFIS model against the identification: a MADALINE model as a generalised multilinear reference model [45], and a Fuzzy Stochastic Neural Network as a reference to model oscillatory dynamics [39]. At this same stage, aiming to evaluate the performance of the proposed model against the SRFJs online control, we implemented an additional Self-Tuned PID Control as an advanced model for controlling complex systems [46].

The performance of the SF-ANFIS model at both the identification and the control stages was made using a fuzzy model proposed by [56]. This model integrates seven statistical metrics to evaluate the behaviour of models by adaptation against error about the SetPoint (SP). In the final stage, a subset of these statistical metrics was used to evaluate the cancellation of oscillations in OPCDs.

4.2. Dynamic Modelling of the System

Based on the RFJs' structure (Figure 2), one dynamic is defined by the movements of the joints in a wide range of operations (main dynamic), while the flexible joints generate the second dynamic in OPCDs, points at which the system becomes oscillatory. This makes RFJs into stochastic robots with flexible joints (SRFJs). The main dynamic is modelled by the Lagrange equation as defined in Annex 1 (7) [57]

Eq.(1) and (2) describe the behaviour of the main dynamics

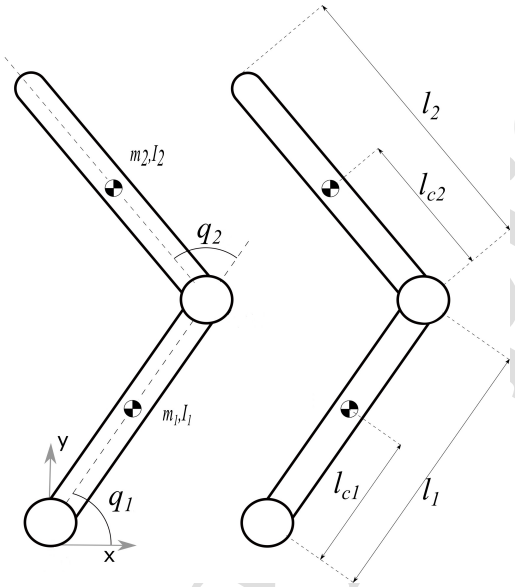

Figure 2: Serial robot with two articulations (main dynamic - main subsystem).

$$\begin{aligned}\tau_1 &= \left(m_1 l_{c_1}^2 + m_2 l_1^2 + m_2 l_{c_2}^2 + 2m_2 l_1 l_{c_2}\cos(q_2) + I_1 + I_2\right)\ddot{q}_1 + \\ &+ \left(m_2 l_{c_2}^2 + m_2 l_1 l_{c_2}\cos(q_2) + I_2\right)\ddot{q}_2 - \\ &- 2m_2 l_1 l_{c_2}\sin(q_2)\,\dot{q}_1\dot{q}_2 - m_2 l_1 l_{c_2}\sin(q_2)\,\dot{q}_2^2 + \\ &+ (m_1 l_{c_1} + m_2 l_1)\,g\sin(q_1) + m_2 g l_{c_2}\sin(q_1+q_2) + f_{1f}\dot{q}_1, \end{aligned} \quad (1)$$

$$\begin{aligned}\tau_2 &= \left(m_2 l_{c_2}^2 + m_2 l_1 l_{c_2}\cos(q_2) + I_2\right)\ddot{q}_1 + \\ &+ \left(m_2 l_{c_2}^2 + I_2\right)\ddot{q}_2 + m_2 l_1 l_{c_2}\dot{q}_1^2\sin(q_2) + \\ &+ m_2 g l_{c_2}\sin(q_1+q_2) + f_{2f}\dot{q}_2, \end{aligned} \quad (2)$$

where $\ddot{q}_1$ and $\ddot{q}_2$ are the second derivatives of q_1 and q_2, respectively; g is the gravitational constant; m_1, m_2 are the mass of the joints (kg); l_{c_1}, l_{c_2} are the centre of mass for each joint (m); l_1, l_2 are the length for each joint (m); $q_1, q_2 \in \left[-\frac{\pi}{4}, \frac{\pi}{4}\right]$ are the angles for each joint (rad); $\dot{q}_1, \dot{q}_2$ their angular velocities; I_1, I_2 are the momentum for each of the bars $(kg.m^2)$; τ_1, τ_2 are

the torque for each joint ($N.m$); and f_{1f}, f_{2f} are the viscosity coefficient for each Joint ($N.m - seg$). These signals are defined in the Table 1. *Signal 1*:τ_1 and *Signal 2*:τ_2 determine the active dynamics of the SFRJs system, while *Signal 3* and *Signal 4* represent two delayed sinusoidal signals to activate the OPCDs' dynamics or passive dynamics. The constants, parameters, and variables are defined in Annex 2 (8) at the end of this document.

Table 1: Identification Signals - System Identification

Signal	**Amplitude** (A)	**Frequency** (rad/s)	**Time Delay** (ms)
1	$\pi/4$	$0.01 \cdot 2 \cdot \pi$	0
2	$\pi/4$	$0.015 \cdot 2 \cdot \pi$	0
3	$\pi/4$	$0.01 \cdot 2 \cdot \pi$	12.500
4	$\pi/4$	$0.015 \cdot 2 \cdot \pi$	8.333

According to Euler-Lagrange equations, the oscillatory dynamics are defined by the compression of the springs in OPCDs, stopping points, or by the effect of the whole system's inertia or collisions. These dynamics can be expressed assuming independence between oscillations in each joint. In this way, the oscillatory dynamics can be described as in Annex 1 (7).

Figure 3 shows the overall response of the SRFJs system. Here, it can be seen that the cross-point between *Signal 1* and *Signal 3* ($1 - joint$), and *Signal 2* and *Signal 4* activate the passive dynamics in OPCDs (system disruption). Integrating the aforementioned dynamics (e.g. main dynamic - OPCDs) allows the creation of a novel modelling methodology for oscillatory dynamics, tackling the stochastic complex systems using Euler Lagrange equations in modelling SRFJs [44, 58]. The identification and control process was defined for 400 seconds, while the sampling was defined by the hardware that supports the Quanser robot ($2ms$).

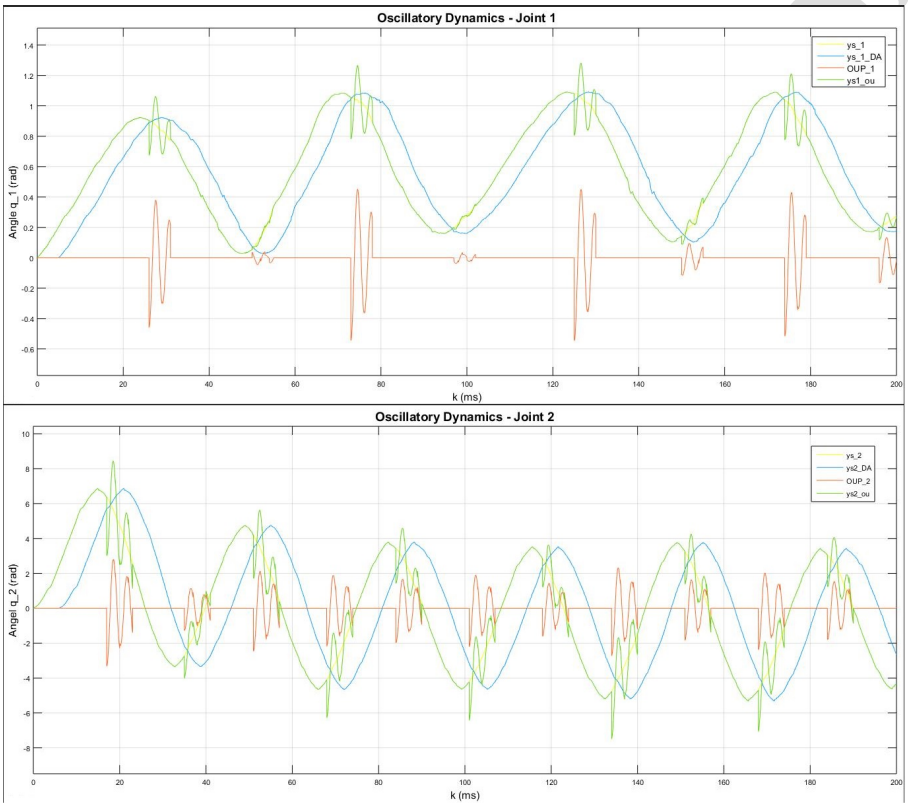

Figure 3: Oscillatory Dynamics - *1-joint* - *2-joint*. The green line, ysi_ou, represents the overall system response for l_i. The blue line, ysi_DA, represents the delayed sinusoidal signal that activates the passive oscillatory dynamics at the OPCDs. The crossover point between the signals that determine the start of oscillatory dynamics is represented by the red line - OUP

Figure 4 shows the overall system response for l_1. As can be seen, and according to Eq. (45), a higher amplitude of the delayed signal after the crossover point generates a greater magnitude and persistence of the oscillations due to the effect of higher torsional inertia in OPCDs.

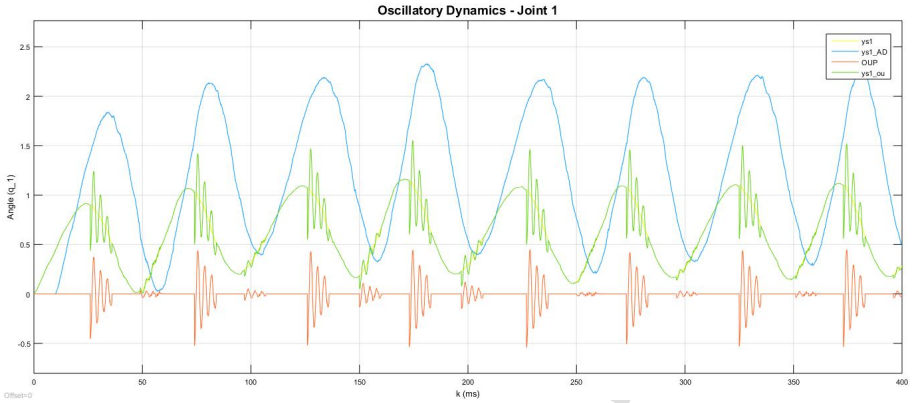

Figure 4: General response of *1-joint* for sinusoidal signals - activation of the passive dynamics. The green line, $ys1\_ou$, represents the overall system response for l_1. The blue line, $ys1\_DA$, represents the delayed sinusoidal signal that activates the passive oscillatory dynamics at the OPCDs. The crossover point between the signals that determine the start of oscillatory dynamics is represented by the red line - OUP

4.3. SF-ANFIS Model

The structure of the proposed SF-ANFIS model is described in the following sections.

4.3.1. General Structure of the Identification Model - Main Dynamics

According to the subsystems that make up an SRFJs model, the structure of the proposed SF-ANFIS model without oscillatory dynamic is denoted and defined by Eq. (3) [59]

$$yr_{l,k} = \sum_{j=1}^{n_o} \sum_{i=1}^{n_i} hn_{l,j} \left(c_{l,j,i} x_{i,k}\right), \tag{3}$$

where $yr_{l,k}$ is the output value for the $l - joint$, l is the number of joints ($l = 1, 2$), j is the number of membership functions ($j = 1, 2, 3, \ldots, n_o$), i is the is input value ($i = 1, 2, 3, \ldots, n_i$), $c_{l,j,i}$ is the output combination supports, k are the time instants (ms), $x_{i,k}$ the input array that describes the system dynamics (Eq. (7)), and $hn_{l,j}$ is the normalised j-membership value, as in Eq. (4)

$$hn_{l,j} = \frac{h_{l,j}}{S_{l,n}}, \tag{4}$$

with $S_{l,n}$ the consolidated sum of the j-membership values for l-joint (Eq. (7)), and $h_{l,j}$ the j-membership value given by Eq. (5)

$$h_{l,j} = exp\left(-\frac{1}{2}\left(\frac{XC_{l,j,i} - x_{i,k}}{D_{l,j}}\right)\right), \tag{5}$$

where $XC_{l,j,i}$ is the j-membership function, i is the input variable for the l-joint, and $D_{l,j}$ the size of a j-membership function.

$$\begin{aligned} x_k &= [x_{1,k}, x_{2,k}, \ldots x_{i,k}, \ldots] \\ &= [q_{11}, q_{12}, \ldots, q_{1,np_1}, e_{11}, e_{12}, \ldots, e_{1,np_2}, u_k, q_{21}, q_{22}, \ldots, \\ &\quad \ldots, q_{2,np_3}, e_{21}, e_{22}, \ldots, e_{2,np_4}, u_{1,k}], \end{aligned} \tag{6}$$

with $q_{l,np}$ the angle for the l-joint taking as reference np delays; np_1, np_2 the numbers of delays for q_{1,np_1}, q_{2,np_2}; e_{1,np_2},e_{2,np_4} describe the error regarding the SP for the l-joint; np_2, np_4 the number of delays for error; k is the discrete-time variable; and u_l is the signal of the control of l-joint.

The number of delays can be obtained from the *auto-correlated*, and *partial auto-correlated* analysis for each angle using the Box and Jenkins methodology [60].

Finally, $S_{l,n}$, the consolidated sum of the j-membership values for l-joint could be found by Eq.(7)

$$S_{l,n} = \sum_{j=1}^{n_o} h_{l,j}. \tag{7}$$

For the particular case of this coupled system (SRFJs), the SF-ANFIS model will take the structure of a coupled auto-regressive media average process
$C - ARMA\,(np_1, np_2, np_3, np_4)$.

4.3.2. General Structure of the Identification and Control Model

The SF-ANFIS model for the identification and control of complex stochastic systems can be expressed as in Eq. (8)

$$yr_{l,k} = \sum_{j=1}^{n_o}\left(\sum_{i=1}^{n_i} hn_{l,j} L_{l,j}\right) + Lou_{l,j}, \tag{8}$$

with $L_{l,j}$ is the internal structure that represents the active dynamics of the system (Eq. (9)), and $Lou_{l,j}$ the set of l-stochastic processes for cancellation of oscillations due to the effect of passive dynamics (Eq. (10)).

$$L_{l,j} = c_{l,j,i} x_{i,k}, \tag{9}$$

$$Lou_{l,j} = f\left(qs_l\right) qou_{l,j}, \tag{10}$$

where $f\left(qs_l\right)$ is a bi-valued function to activate the passive dynamics (Eq. (12)), and $qou_{l,j,k}$ represents the discretized OU process with mean reversion. Formally, an Ornstein-Uhlembeck process describes the velocity of a cloud of Brownian Particles under the influence of friction over time. This process tends to drift towards its long-term mean, i.e. mean-reversion. In general, the OU process can be considered a modification of random walk in continuous time, a Weiner process, and a continuous version of the discrete-time AR(1). The oscillatory dynamics are denoted and defined as in Eq. (11) [61]

$$qou_{l,j,k} = qou_{l,j,k-1} + \theta_l \left(SP_l - qou_{l,j,k-1}\right) .\triangle k + \sigma_l . \sqrt{\triangle k} . randn, \tag{11}$$

with θ_l the rate of reversion to the mean or SP for l-joint, SP_l the SetPoint for l-joint, σ_l the amplitude of oscillations for l-joint, and $\sqrt{\Delta k}.randn$ the persistence of the oscillations in OPCDs based in a slow Wiener process. The random values are defined by the distribution $\mathcal{N}\left(0, 1\right)$. Finally, the function $f\left(qs_l\right)$ is defined by Eq. (12)

$$f\left(qs_l\right) = \begin{cases} 1 & \|qs_l\| >= SP_l \\ 0 & \|qs_l\| < SP_l \end{cases}, \tag{12}$$

where qs_l represents the crossing point between sinusoidal input signals (Section 4.2).

4.3.3. Identification Process - Active Dynamics

The configuration of the proposed SF-ANFIS model in the stage of Active Dynamic ($f\left(qs_l\right) = 0$) is defined by the GDR, which is represented by the Eq.(13), (14), and (15) [45]

$$c_{l,j,i,k} = c_{l,j,i,k-1} - \alpha_l \frac{\partial e^2_{l,k-1}}{\partial c_{l,j,i,k-1}}, \tag{13}$$

$$XC_{l,j,i,k} = XC_{l,j,i,k-1} - \alpha_l . \frac{\partial e^2_{l,k-1}}{\partial XC_{l,j,i,k-1}}, \tag{14}$$

$$D_{l,j,k} = D_{l,j,k-1} - \alpha_l . \frac{\partial e^2_{l,k-1}}{\partial D_{l,j,k-1}}, \tag{15}$$

where α_l is the learning factor and $e^2_{l,k}$ is the mean square error for each l-joint given by Eq. (16)

$$e^2_{l,k} = \frac{1}{2}\left(yd_{l,k} - ys_{l,k}\right)^2, \tag{16}$$

with $yd_{l,k}$ the SP or reference angle for l-joint and $yr_{l,k}$ the response of the l-joint subsystem identification model.

According to the structure that defines the SF-ANFIS model, Eq. (17), (18) and (19) allow for the updating of the model structure

$$c_{l,j,i,k} = c_{l,j,i,k-1} + \alpha_l e_{l,k} hn_j x_{i,k}, \tag{17}$$

$$XC_{l,j,i,k} = XC_{l,j,i,k-1} + \alpha_l e_{l,k} \frac{h_{j,k}}{S_{l,n}} \left(\frac{x_{i,k} - XC_{l,j,i,k-1}}{\sigma^2_{j,k}} \right) L_{l,j}, \tag{18}$$

$$D_{l,j,k} = D_{l,j,k-1} + \alpha_l e_{l,k} \frac{h_{j,k}}{S_{l,n}} \left(\frac{\sum_i \left(XC_{l,j,i,k} - x_{i,k} \right)}{\sigma^2_{j,k}} \right) L_{l,j}. \tag{19}$$

Importantly, the passive structure of the model, $Lou_{l,j}$, only intervenes in the cancellation of oscillations in OPCDs as an independent term within the control process.

4.3.4. Adaptive Stochastic Control

According to the structure of the SF-ANFIS model (Eq. (8)), the model integrates into a single structure two algorithms, one based on the GDR for the control of active dynamics, while for control and stabilisation in OPCDs, the model integrates an EDA based on Multi-dynamics Algorithm for Global Optimisation (MAGO) [28].

In general, the adaptive stochastic control for the active dynamics is defined by the GDR ($L_{l,j}$, $f\left(qs_l\right) = 0$), and is denoted and defined by Eq. (20)

$$u_{l,k} = u_{l,k-1} - \rho l \frac{\partial e_{l,k}}{\partial u_{l,k-1}}, \tag{20}$$

where $u_{l,k}$ is the signal of control for the l-joint, and ρ_l is the stability factor. Eq. (20) can be rewritten as Eq. (21)

$$u_{l,k} = u_{l,k-1} + \rho_l e_{l,k} . \frac{h_{j,k}}{S_{l,n}} \left(\frac{x_{u_l,k} - XC_{l,j,u_l,k}}{\sigma^2_{j,u_l,k}} \right) L_{l,j} + \rho_l e_{l,k} h n_j L_{u_l,k} + Lou_{l,j}, \tag{21}$$

with $x_{u_l,k}$ the component of signal control, $XC_{l,j,u_l,k}$ the j-membership value for u_l control signal. It is important to emphasise that the term passive $Lou_{l,j}$ only intervenes for the cancellation of the oscillations ($f(qS_l) = 1$). $L_{ul,k}$ is the control component related to SF-ANFIS output that can be defined according to Eq. (22)

$$L_{u_l,k} = c_{l,j,i,k} \frac{\partial x_k}{\partial u_l}. \tag{22}$$

The active part of the control can be expressed as in Eq. (23)

$$L_{act,l} = \frac{h_{j,k}}{S_{l,n}} \left(\frac{x_{u_l,k} - XC_{l,j,u_l,k}}{\sigma^2_{j,u_l,k}} \right) L_{l,j} + h n_j L_{u_l,k}. \tag{23}$$

4.3.5. Passive Control Stage - Oscillatory Dynamics

The passive dynamics is defined by oscillatory dynamics, which is activated by a crossing point between two sinusoidal delayed signals as shown in Figure 4 and defined by the Eq. (45). The amplitude of the sinusoidal delayed signal (*Signal 3, Signal 4*) represents the magnitude and persistence of the oscillations in the OPCDs ($f\left(qs_l\right) = 1$). In this stage, the control has the structure defined by Eq. (24), according to the SF-ANFIS structure.

$$u_{l,k} = u_{l,k-1} + \rho_l e_{l,k} . \left(L_{act,l}\right) + Lou_{l,j}. \tag{24}$$

The parameters that define a j-stochastic process (Eq.(11)) will be configured dynamically using an EDA inspired in a MAGO model [28]. According to the general structure of the $Lou_{l,j}$, the structure of individual is denoted and defined by Eq.(25)

$$x_{Il} = [\rho_{1,l}, \quad \rho_{2,l}, \quad \theta_{1,l}, \quad \sigma_{1,l}, \quad \theta_{2,l}, \quad \sigma_{2,l}], \tag{25}$$

where x_{Il} are the components or gens that defines the whole j-stochastic process ($x_{I,i} \sim \mathcal{N}(0,1)$), and ρ_l represents the strength in the cancellation of the oscillations for l-joint. For the stabilisation of the system in this stage, the evolutionary model starts with a uniform random distribution population with n_i individuals or solutions. The fitness function (f) that defines the quality for each individual is defined as in Eq. (26)

$$f = \frac{kou}{\sum_{k=1}^{nd} e_{l,k}^2}, \tag{26}$$

with kou the scaling constant to avoid the explosion of decimals, and nd the number of data that make up the window for modeling the oscillatory dynamics.

The evolutionary model that transforms the possible solutions or individuals is performed by creating new individuals from three operators: Emergent Dynamics, Crowd Dynamics, and Accidental Dynamics. For this control, the two first dynamics were used to stabilise the model in real-time. The first operator is responsible for creating and selecting an elite or the best individuals in agreement with the f. The creation of a new individual using this operator is defined as in Eq. (27) [28]

$$x_{I,i}^{(k)} = x_{I,i}^{(k-1)} + F^{(k-1)} \left(x_{I,i_B}^{(k-1)} - x_{I,i_m}^{(k-1)} \right), \tag{27}$$

where $x_{I,i}^{(k)}$ is a new i individual for the k-window, $x_{I_{i,B}}^{(k-1)}$ is the best individual), and $x_{I_{i,m}}^{(k-1)}$ is the average individual. Regarding $F^{(k-1)}$, represents the current relations between the individuals (e.g., Index of Agreement). The $F^{(k-1)}$ relationship is defined by Eq. (28)

$$F^{(k-1)} = \frac{S^{(k-1)}}{\|S^{(k-1)}\|}, \tag{28}$$

where $S^{(k-1)}$ is the sample covariance matrix of the individual's population in the $k-1$ instant and $||,||$ is the norm operator.

The second operator used to stabilise the system is defined by Crowd Dynamics. This operator has the role of exploring the space of solution around the population's mean, avoiding the dispersion of solutions and compressing

the $e_{l,k}^2 \approx 0$. The creation of new individuals in the Crowd Dynamics is defined by sampling from a uniform distribution in the hyper-rectangle given by Eq. (29)

$$\left[LB_i^{(k)}, UB_i^{(k)}\right], \tag{29}$$

with $LB_i^{(k)} = x_{i,m}^{(k)} - \sqrt{DS_i^{(k)}}$, for the m-th individual; $UB_i^{(k)} = x_{i,m}^{(k)} + \sqrt{DS_i^{(k)}}$; and $DS_i^{(k)}$ is the dispersion vector for each i gen in the population of n individuals, given by Eq.(30)

$$DS^{(k)} = \left[DS_1^{(k)} \quad DS_2^{(k)} \quad \dots \quad DS_n^{(k)}\right]. \tag{30}$$

The evolutionary stabilisation process in the passive learning stage is defined by the Algorithm 1.

Algorithm 1 Multi-dynamics algorithm - Oscillatory dynamics

1: Initiation of the passive learning - operational point with the change of direction
2: Initial population - random sampling
3: Evaluate each individual in agreement with the fitness function
4: **repeat**
5: $k1 = 0$
6: **repeat**
7: Select the best individual in agreement with the fitness function
8: Calculate the sample co-variance matrix $S^{(k_1)}$
9: Modify the best individual in agree with the Eq.(29)
10: Create a new individual from a distribution $\left[LB_i^{(k)}, UB_i^{(k)}\right]$.
11: Select the best individual, and eliminate the worst individual from the population.
12: $k1 = k1 + 1$
13: **until** $k1 <= 10$
14: **until** ending the oscillatory dynamics.

4.3.6. Study Case - SF-ANFIS Adaptive Control

According to the general structure of the SF-ANFIS model, and in agreement with the Box and Jenkins methodology [60], the proposed model can be

represented in a basic form as a coupled ARMA model or $C-ARMA(np_1, np_2, p_3, np_4)$ model, where the np_1, np_3 values represent the auto-regressive behaviour of the system (auto-regressive degree). In contrast, the np_2, np_4 values represent the number of times to cancel the oscillatory dynamics defined for each l-joint (error degree). For this specific study case, the structure of the model is defined as a $C-ARMA(1,1,1,1)$, where the structure of the input vector can be expressed as Eq. (31)

$$x_k = [q_{1,k} \quad e_{1,k} \quad u_{1,k} \quad q_{2,k} \quad e_{2,k} \quad u_{2,k} \quad f(q_{s1})\, qou_{1,k} \quad f(q_{s2})\, qou_{2,k}], \quad (31)$$

where the vector x_k represents the input values for the angles ($q_{1,k}$, $q_{2,k}$), the errors with regard to the SP or reference operation ($e_{1,k}$, $e_{2,k}$), and the oscillatory dynamics ($qou_{1,k}$, $qou_{2,k}$) for each l-joint. Table 2 shows the fuzzy sets that make up the linguistic variables for the angles ($XC_{l,j,i,k}$, $\sigma_{l,j}$), and the fuzzy sets that make up the linguistic variables for control signals ($XC_{j,u,i,k}$, $\sigma_{j,u,i,k}$). In general, the linguistic variables are defined by the operating angles of the system ($[-2\pi, 2\pi]$).

Table 2: Fuzzy sets that define the input variables for each j-joint

	Min	**Very Low**	**Low**	**Medium**	**High**	**Very High**	**Max**
$\mathrm{XC}_{l,j,:,k}$	-0.78	-0.31749	-0.14064	-0.02799	0.13933	0.36400	0.78
$\sigma_{l,j,:,k}$		0.31968	0.14475	0.13998	0.19599	0.32033	
$\mathrm{XC}_{u_l,j,:,k}$	-1.2	-0.48928	-0.22295	-0.02691	0.15265	0.38341	1.2
$\sigma_{u_l,j,:,k}$		0.48852	0.23118	0.18779	0.20516	0.52367	

Figure 5 and Table 3 shows the whole behaviour after 13 secs. of operation. Table 3 also shows that the oscillatory dynamics is active for 2-joint ($f(q_{s1}) = 1, qou_{2,k} = 0.0116$), due to the oscillations that presents with regard the $SP_{2,k}$.

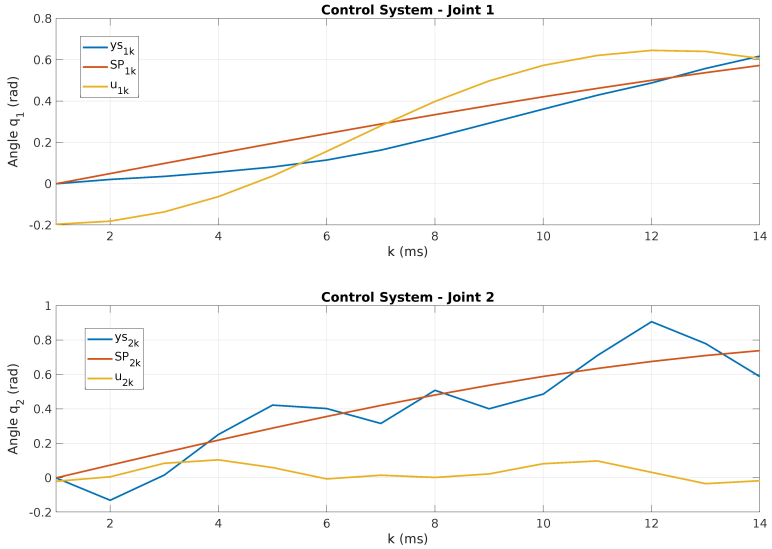

Figure 5: System status after 13 secs of operation for *1-joint* and *2-joint*

Table 3: System behaviour

Input Variables - System Behaviour				
$q_{1,k}$	$u_{1,k}$	$e_{1,k}$	$f(q_{s1})$	$qou_{1,k}$
0.52230	0.53830	-0.03583	0	0.02346
$q_{2,k}$	$u_{2,k}$	$e_{2,k}$	$f(q_{s2})$	$qou_{2,k}$
0.89430	0.12670	-0.01363	1	0.0116

In the first stage of control implementation, we proceeded to generate a total of 5-membership functions taking as a reference the number of input variables according to Table 3, the structure of vector x_k and $C-ARMA(1,1,1,1)$. These j-memberships were randomly generated based on the values shown in Table 2.

The output values associated with each of the j-membership functions ($h_{j,k}$) and their subsequent normalisation ($hn_{j,k}$) can be expressed as in Eq. (32) and (33)

$$h_{j,k} = \exp\left(-\frac{1}{2}\left(\frac{XC_{j,i,k} - x_{i,k}}{D_{j,i}}\right)^2\right), \tag{32}$$

$$h_{j,k} = \begin{bmatrix} 0.89640 \\ 0.76228 \\ 0.92067 \\ 0.77806 \\ 0.53629 \end{bmatrix}, hn_{j,k} = \begin{bmatrix} 0.23021 \\ 0.19577 \\ 0.23644 \\ 0.19982 \\ 0.13773 \end{bmatrix}. \tag{33}$$

The output value estimated for each joint according to the structure of the model can be expressed as in Eq. (34)

$$L_{l,j} = c_{l,j,i,k} x_{i,k}, \tag{34}$$

where $c_{l,j,i,k}$ is an array of uniform random numbers generated in the interval $[-1, 1]$. The final parameters used for the first stage are shown in Eq. (35)

$$L_{l,k} = \begin{bmatrix} 0.56180 \\ 0.58943 \end{bmatrix}, SP_{l,k} = \begin{bmatrix} 0.57251 \\ 0.73958 \end{bmatrix}, e_{l,k} = \begin{bmatrix} 0.01071 \\ 0.15015 \end{bmatrix}. \tag{35}$$

For the cancellation of oscillations in the second stage, we proceeded with the creation of possible solutions or individuals according to MAGO algorithm (Eq.(27)). Table 4 shows, as an example, two individuals created, individual 1 (I_1) and individual 2 (I_2). According to the emergent dynamics, we can create a new individual, $I_{1,2}$, from these two individuals. This exact procedure applies to all the individuals created at this stage.

Table 4: New individual - Emerging dynamics ($F^{(k-1)} = -0.78488$)

Ind	ρ_1	ρ_2	θ_1	σ_2	θ_2	σ_2	f
I_1	−0.04572	−0.05135	−0.08105	0.00709	−0.00120	0.09885	0.39155
I_2	0.03784	0.04906	0.03211	0.02320	−0.09113	−0.09955	3.47947
$I_{1,2}$	−0.02775	−0.02875	−0.05671	0.01055	−0.02054	0.05617	2.78956

In the third stage, we proceeded with updating the control signals. For 1-joint ($f(q_{s1}) = 0$) the update was carried out taking as reference the Eq. (26), resulting in Eq. (36)

$$
\begin{aligned}
u_{1,k} &= u_{1,k-1} + \rho_1 e_{1,k} \frac{h_{j,k}}{Sn_k} \left(\frac{x_{u_1,k} - XC_{1,j,u_1,k}}{\sigma^2_{j,u_1,k}} \right) L_{1,k} + \rho_1 e_{1,k} hn_j L_{u_{1,k}} + Lou_{1,j,k}, \\
0.5383 &= 0.5383 - \left(0.0277 \cdot 0.0107 \cdot 3.8937 \cdot \begin{bmatrix} 0.0007 \\ 0.0106 \\ -0.0022 \\ 0.0015 \\ 0.0293 \end{bmatrix}^T \cdot \begin{bmatrix} 0.5466 \\ -0.0068 \\ -0.8418 \\ -0.3976 \\ 0.8093 \end{bmatrix} \right) - \\
&\quad - \left(0.0277 \cdot 0.0107 \cdot \begin{bmatrix} 0.2302 \\ 0.1958 \\ 0.2364 \\ 0.1998 \\ 0.1377 \end{bmatrix}^T \cdot \begin{bmatrix} 0.3568 \\ 0.1319 \\ -0.6809 \\ 0.3993 \\ -0.7630 \end{bmatrix} \right) + 0. \qquad (36)
\end{aligned}
$$

For 2-joint ($f\left(q_{S2}\right) = 1$), the signal control update was made taking into account the cancellation of oscillations based on the parameters provided by the *Emergent Operator* (Eq.(29)) defined by the MAGO algorithm (Table 4). The results are shown in Eq. (37)

$$
\begin{aligned}
u_{2,k} &= u_{2,k-1} + \rho_2 e_{2,k} \frac{h_{j,k}}{Sn_k} \left(\frac{x_{u_2,k} - XC_{2,j,u_1,k}}{\sigma^2_{j,u_2,k}} \right) L_{2,k} + \rho_2 e_{2,k} hn_j L_{u_{2,k}} + Lou_{2,j,k} \\
0.13887 &= 0.12670 + \left(0.0297 \cdot 0.0136 \cdot 3.8937 \cdot \begin{bmatrix} 0.0077 \\ 0.0291 \\ 0.0058 \\ 0.0157 \\ -0.0058 \end{bmatrix}^T \cdot \begin{bmatrix} 0.0743 \\ 0.2933 \\ -0.5077 \\ -0.4325 \\ 0.6899 \end{bmatrix} \right) + \\
&\quad + \left(0.0297 \cdot 0.0136 \cdot \begin{bmatrix} 0.2302 \\ 0.1958 \\ 0.2364 \\ 0.1998 \\ 0.1377 \end{bmatrix}^T \cdot \begin{bmatrix} -0.5999 \\ 0.9234 \\ 0.6978 \\ 0.7542 \\ -0.5783 \end{bmatrix} \right) + (0.1160 - 0.0205) \cdot \\
&\quad \cdot (0.7396 - 0.0116) \cdot 0.002 + 0.0100 \cdot 0.0447 \cdot 1.1152. \qquad (37)
\end{aligned}
$$

In general, the operators grouped by the MAGO Algorithm 1 were used randomly to update the control signals during the entire operation of SRFJs.

4.4. Experimental Evaluation

We considered three stages for the analysis and evaluation of the SF-ANFIS model. The first stage focuses on the identification process, where the proposed model was set up using two learning strategies: a first learning strategy based on a GDR algorithm ($yr_{l,3}$) [62], and a second learning strategy based on EDA algorithm ($yr_{l,4}$) for modelling the oscillatory dynamics. In this stage, we evaluated the proposed model against MADALINE ($yr_{l,1}$) and a Fuzzy Stochastic Neural Network as an adaptive reference model for the identification of stochastic systems ($yr_{l,2}$) [39]. The structure of the input array (x_k) was defined by the auto-correlation (DAC) and partial auto-correlation diagrams (DACP) [63]. The second stage focuses on the control process, where the SF-ANFIS model was set up using the two learning strategies defined in the first stage (GDR - EDA). The SF-ANFIS proposed model was evaluated against three different controllers, the two adaptive models used in the identification stage ($yr_{l,1}$, $yr_{l,2}$), and an additional model based on a self-tuning PID control ($yr_{l,PID}$) [46]. In the third stage, we evaluated the SF-ANFIS model against the persistence and cancellation of the oscillations in OPCDs.

4.4.1. Fuzzy Statistics Model

For the analysis and general evaluation of the SF-ANFIS model in the different stages, the fuzzy model proposed by [56] was used. This fuzzy model integrates seven statistical metrics to evaluate the performance of adaptive models against the error (ek_l). The statistical indices are the following: fractional bias (FB), normalised mean square error (NMSE), geometric bias mean (MG), geometric bias-variance (VG), within a factor of two (FAC2), index of agreement (IOA), unpaired accuracy of peak (UAPC2) and mean relative error. This model also proposes a series of values that are additive according to the qualities which define the statistical indices as linguistic variables: Good 7-10 (average 8.5), Fair 4-7 (average 5.5), Over Fair (average 6), Under Fair (average 5) and Poor 1-4 (average 2.5) as shown the Eq. (38)

$$Score = \sum_{i=1}^{nmt} q(FS_i), \tag{38}$$

where $i \in \{1,2, \ldots, 8\}$ refers to the eight metrics {FB,NMSE, GBM, GBV, FAC2, UAPC, MRE, IOA}, $nmt = 8$ is the number of metrics, FS_i is the scale value for the i-metric {Good, Fair, Over Fair, Under Fair, Poor}, and q is the value associated to each quality {8.5, 5.5, 6,5, 2.5}.

According to this fuzzy statistical model, FB shows the over and sub estimation concerning an SP (SP_l), and NMSE determines the normalised error. MG shows the discrepancies of the means between the model and the SP, VG shows the oscillations of the model around the SP, UPAC2 shows the difference between maximum values of reference, FAC2 determines the system variation between 80% and the 120% of the SP, IOA shows the relationships between forms of the curves that represent the response of the system and the SP. In contrast, MRE shows the relative error to reach the SP (SP_l).

To evaluate the behaviour of the model in the cancellation of oscillations in OPCDs, we use four statistical indices of the fuzzy proposed model: NMSE (Normalised Magnitude of the Error), MG (Mean of Oscillations), VG (Maximum Magnitude of Oscillations in a similar way of NMSE), and the UAPC2, which shows the persistence of oscillations along the time.

5. Results

We considered three stages for the analysis and validation of the proposed SF-ANFIS model: a first identification stage or setting SF-ANFIS model, a second stage defined by the adaptive control process, and a final stage or cancellation of oscillations.

5.1. Identification Stage

Table 5 and Figure 6 show that the MADALINE model achieved the best statistical indices in the stage of identification for 1-joint (yr_{11}), among which it highlighted the IOA (0.9975), UAPC2 (0.0006) and VG(1.0091), followed by the SF-ANFIS model with an IOA (0.8785), UAPC2 (-0.0084) and VG(1.0188). The SF-ANFIS response tends to be located below the SP as corroborated by the FB (0.0400). This behaviour clearly shows that the structure of the SF-ANFIS model ((yr_{14})) has to round the response by the effect of the structure of the membership functions, which makes it ideal for the control of complex systems with oscillatory behaviours or unstable systems.

Table 5: Statistical indices to evaluate the model - Identification stage

Joint 1								
	yr11		**yr12**		**yr13**		**yr14**	
FB	0.0217	G	0.0466	G	0.0996	G	0.0400	G
NMSE	0.0047	G	0.0182	G	0.0302	G	0.0131	G
MG	1.0253	G	1.0569	G	1.1059	G	1.0469	G
VG	1.0091	G	1.0318	G	1.0324	G	1.0188	G
FAC2	0.9975	G	0.9825	G	1.0000	G	0.9900	G
IOA	0.9511	G	0.8339	G	0.7640	G	0.8785	G
UAPC2	0.0006	G	-0.0003	G	0.0186	G	-0.0084	G
MRE	0.0212	G	0.0433	G	0.0863	G	0.0380	G
Score		68		68		68		68
Joint 2								
	yr21		**yr22**		**yr23**		**yr24**	
FB	0.0080	G	0.0082	G	-0.0018	G	0.0067	G
NMSE	0.0017	G	0.0023	G	0.0025	G	0.0016	G
MG	1.0065	G	1.0062	G	0.9970	G	1.0045	G
VG	1.0011	G	1.0015	G	1.0037	G	1.0012	G
FAC2	1.0000	G	1.0000	G	1.0000	G	1.0000	G
IOA	0.9953	G	0.9934	G	0.9927	G	0.9955	G
UAPC2	0.0001	G	-0.0004	G	-0.0005	G	-0.0003	G
MRE	0.0059	G	0.0055	G	-0.0049	G	0.0039	G
Score		68		68		68		68

Figure 6 shows the behaviour of oscillations in the stage of online identification. These oscillations were disappearing as the learning became more specialised. The other statistical indices show the good behaviour of the models in this stage in agreement with the score established by [56]. Regarding the control for 2-joint, which presents the greatest oscillations, the SF-ANFIS (yr_{24}) model showed better statistical indices than the MADALINE model, among those that stand out, the IOA (0.9955), VG (1.0012) and UAPC2 (-0.0003), that show equally the tendency of the model to soften the oscillations about 2-joint. The VG index reached by the proposed SF-ANFIS model shows the EDA algorithm's appropriate behaviour in identifying the oscillations by the random sampling that develops the EDA algorithm. Regarding the 2-joint, the models generally reached the maximum score according to the statistical indices established to evaluate the behaviour of the identification models; however, the SF-ANFIS model obtained the best statistical index concerning two joints.

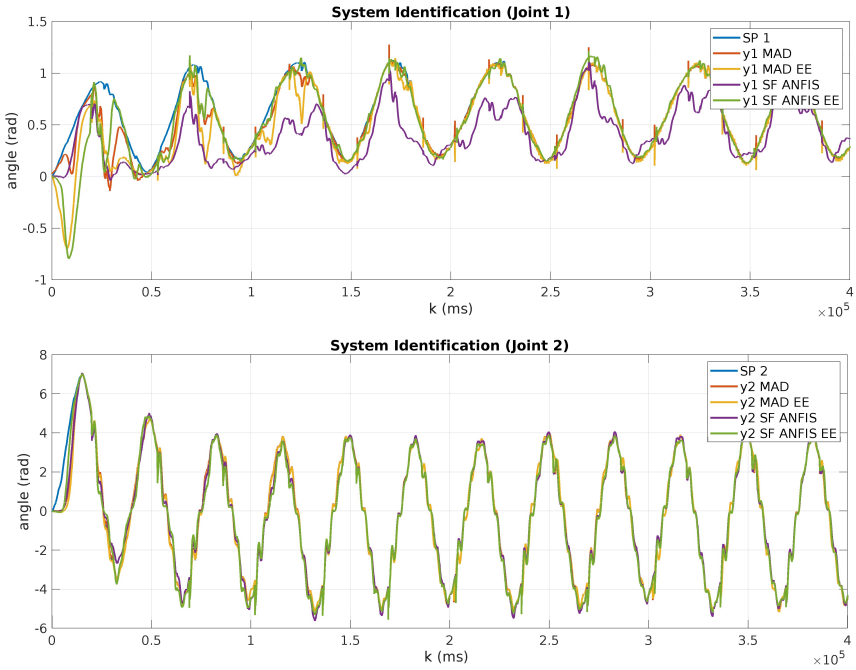

Figure 6: System identification stage

5.2. Control Stage

Table 6 and Figure 7 show the behaviour of the models against the online control process for 1-joint. Here, the Fuzzy Stochastic Model (FSM- $yr_{1,2}$) shows the best results with an IOA (0.9898), MG (1.0027) and VG (1.0012), followed by the SF-ANFIS ($yr_{1,4}$) model with an IOA (0.9801), VG (1.0021) and MG (-0.0031). The value promoted by this good behaviour had been taken by the IOA, MG and VG, which were closed to unity. In general, these control models show the tendency to be located above the SP (q_1), as they show the sign taken by the FB (-0.0004,-0.0013) index, respectively.

Figure 8 shows the behaviour of Lou_l (Eq.(24)) model to cancel oscillations around the SP_1 with minimum persistence. The models used to evaluate the SF-ANFIS model in the control stage for 1-joint showed relevant results. However, the MADALINE model presented a delay concerning the SP_1, as shows the low value achieved by IOA (0.4487), delays that affect the

Table 6: Statistical indices - Control stage

Joint 1										
	yr11		**yr12**		**yr13**		**yr14**		**yr1_PID**	
FB	-0.0157	G	-0.0004	G	-0.0094	G	-0.0013	G	-0.0348	G
NMSE	0.0362	G	0.0001	G	0.0048	G	0.0019	G	0.0048	G
MG	0.9835	G	1.0027	G	0.9946	G	1.0031	G	0.9590	G
VG	1.0402	G	1.0012	G	1.0052	G	1.0021	G	1.0061	G
FAC2	1.0000	G	1.0000	G	1.0000	G	1.0000	G	1.0000	G
IOA	0.4487	F	0.9898	G	0.9424	G	0.9801	G	0.9518	G
UAPC2	-0.0210	G	-0.0280	G	-0.0830	G	-0.0670	G	-0.0460	G
MRE	-0.0366	G	0.0021	G	-0.0080	G	0.0020	G	-0.0450	G
Score		65.5		68		68		68		68
Joint 2										
	yr21		yr22		yr23		yr24		yr2_PID	
FB	-0.0348	G	-0.0034	G	0.0015	G	-0.0003	G	0.0015	G
NMSE	0.0048	G	0.0029	G	0.0034	G	0.0016	G	0.0007	G
MG	0.9590	G	0.9963	G	1.0041	G	1.0008	G	1.0019	G
VG	1.0061	G	1.0033	G	1.0037	G	1.0019	G	1.0007	G
FAC2	1.0000	G	1.0000	G	1.0000	G	1.0000	G	1.0000	G
IOA	0.9518	G	0.9547	G	0.9534	G	0.9766	G	0.9892	G
UAPC2	-0.0460	G	-0.0430	G	-0.1410	G	-0.0460	G	-0.0580	G
MRE	-0.0450	G	-0.0053	G	0.0022	G	-0.0001	G	0.0015	G
Score		68		68		68		68		68

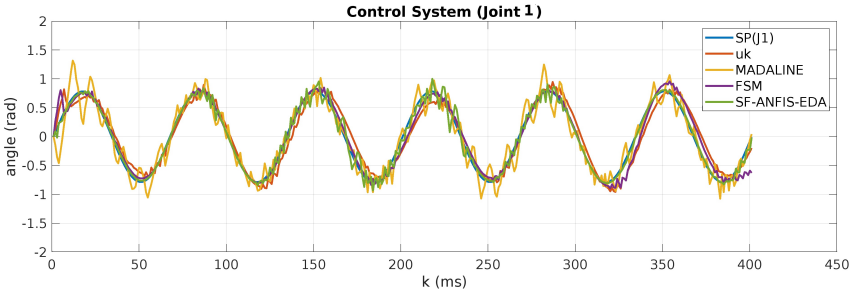

Figure 7: Control stage

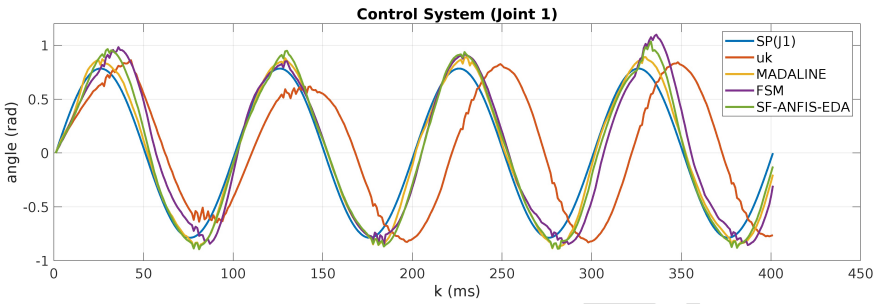

Figure 8: Control stage - Joint 1 - SF-ANFIS model

control accuracy in OPCDs.

Regarding the 2-joint, the models had different behaviours, where the SF-ANFIS (yr_{24}) achieved the best values with an IOA (0.9766), VG (1.0019) and FB (-0.0003), followed by the ST-PID ($yr_{2,PID}$) control with an IOA (0.9892), VG (1.0007) and MG (1.0019). However, against this joint, the ST-PID failed to reach extreme angles according to FB (0.0015), located below (SP_2) by the directional friction that presents this joint. For its part, the MADALINE model ($yr_{2,2}$) shows significant disturbances in the control process concerning this joint, it was reflected in the value that takes the UAPC2 (-0.0430) and as shown in the value taken by the MRE (-0.0450) and FB(-0.0348) indices, in spite the good values reached by this model for both joints (1-joint,2-joint) with regard MG (0.9835,0.9590) and VG (1.0402,1.0061). This behaviour reflects the MADALINE model's instability to cancel RFJ oscillations for RFJs.

The SF-ANFIS model generally showed the best behaviour in the system's control for both joints, thanks to the capacity to identify and cancel oscillations based on the advanced sampling that defines an EDA algorithm. This behaviour significantly differs from the Fuzzy Stochastic Model (FSM). The sampling process does not have a defined structure in agreement with the behaviour that exhibits the joints. However, the FSM and SF-ANFIS models reached the maximum angles for both joints when the signal control was limited to interval $[-1.2A, 1.2A]$, overcoming the limitations imposed by the directional friction and torsional effects presented in the joints. This limitation was also reflected in the behaviour of the ST-PID control, where the response of the system tends to be located below SP_1 ($FB > 0$) and above

SP_2 ($FB < 0$) for maximum values of the control signal.

5.3. Cancellation of Oscillations

Eq. (20), (21), (22), and (24) show how the active and passive learning for the control process carried out the cancellation of oscillations Lou_l in OPCDs. Eq. (39), (40), and (41), show how the global stability is guaranteed by the GAS theorem, and by the behaviour of the error when the stability factor for each joint is defined $\rho_{ou,l} > 0$.

$$\frac{de_k^2}{dt} = \frac{\partial e_k^2}{\partial yr_k}.\frac{\partial yr_k}{\partial u_{l,k}}.\frac{\partial u_{l,k}}{\partial Cou_{l,j,k}}.\frac{\partial Cou_{l,j,k}}{\partial t}, \tag{39}$$

$$\frac{\partial Cou_{l,j,k}}{\partial t} = -\alpha_{l,ou}.\frac{\partial e_k^2}{\partial yr_k}.\frac{\partial yr_k}{\partial u_{l,k}}.\frac{\partial u_{l,k}}{\partial Cou_{l,j,k}}, \tag{40}$$

$$\frac{de_k^2}{dt} = -\alpha_{ou}.e_k^2.\left|\frac{\partial yr_k}{\partial u_{l,k}}\right|^2.\left\|\frac{\partial u_{l,k}}{\partial Cou_{l,j,k}}\right\|^2, \tag{41}$$

where Cou are the weights at the output of the neural network for the OU model.

Figure 8 shows the stability of the SF-ANFIS (yr_{14},yr_{24}) in OPCDs by operating angles $\left\{-\frac{\pi}{4}, \frac{\pi}{4}\right\}$. Figure 9 shows the little persistence of oscillations achieved by the SF-ANIFS model near to this angles ($yc_{ou,1,4}$,$yc_{ou,2,4}$), unlike the persistence of the oscillations and the delay in the response that presents the MADALINE model, thanks to few capacity to cancel the disturbances

Four statistical indices were used to evaluate the behaviour of the models against the cancellation of oscillations in the third stage. Table 7 shows that the SF-ANFIS achieved the best behaviour followed by the MADALINE model, where it is highlighted the UAPC2 (0.9525) value, which indicates that the proposed model reaches a 95.25% of the time the SP_1 established by the 1-joint with minimum persistence. According to the 2-joint, the model achieved the best values regarding the UAPC2 (Joint 1: 0.9450, Joint 2: 0.8825), which corroborates the proper behaviour of the proposed model in the cancellation of oscillations in agreeing to the Lyapunov's global stability. Finally, Figure 10 presents an area indicator, where the coverage or importance of the indices is in relationship with the suitable solution to the problem. Table 7 also shows that the SF-ANFIS model achieves the major area in general, despite the fair behaviour related to the stability of the 2-joint, which once again confirms the proper behaviour of the model.

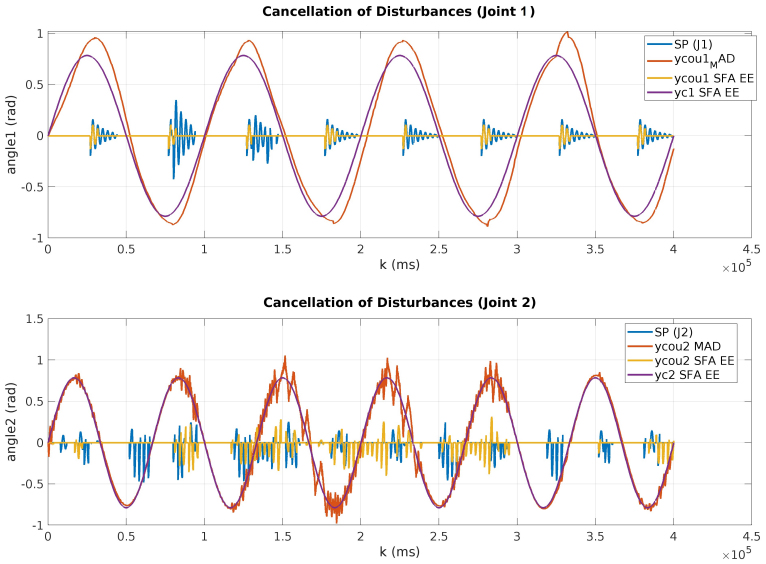

Figure 9: Cancellation of Disturbances (Joint 1) Figure

Table 7: Statistical indices to evaluate the behaviour of the model in the passive learning stage

Joint 1					
	ycou11	**ycou12**	**ycou13**	**ycou14**	**ycou1_PID**
NMSE	0.9780	0.9889	0.9891	0.9848	0.9981
MG	1.0142	1.0064	1.0063	1.0048	1.0048
VG	0.5743	0.5878	0.5879	0.5812	0.5973
UAPC2	0.2075	0.6700	0.6975	0.9525	0.9100
Joint 2					
	ycou21	**ycou22**	**ycou23**	**ycou24**	**ycou2_PID**
NMSE	0.9841	0.9920	0.9992	0.9950	0.9948
MG	1.0238	1.0070	1.0030	1.0014	1.0160
VG	0.5684	0.5960	0.5991	0.5921	0.5925
UAPC2	0.8375	0.6200	0.9450	0.8825	0.8725

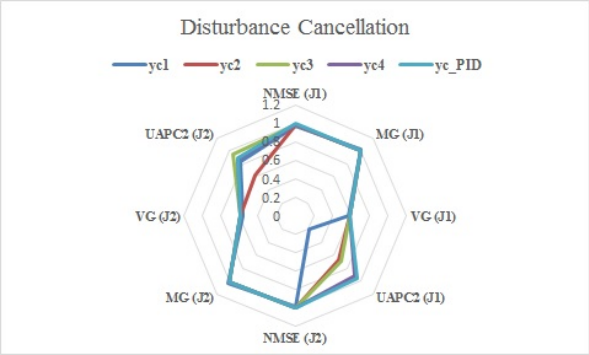

Figure 10: Radar Plot - General behaviour SF-ANFIS model

6. Conclusions and Future Work

This paper presents a novel adaptive, flexible stochastic model SF-ANFIS for online control of coupled systems with stochastic behaviours, as shown in RFJs. The appropriate behaviour was promoted by the effect of the SF-ANFIS in the identification and control stages, thanks to the structure of the fuzzy sets that have the trend to round the oscillatory response of the systems in OPCDs. This behaviour was extended to the control stage, making the model ideal for controlling systems with stochastic and oscillatory behaviours in different operational points or trajectories.

We achieved the theoretical modelling of the RFJs by integrating the Euler Lagrange of two sinusoidal delay signals to model the persistence of the disturbances in OPCDs, setting a novel methodology to model stochastic behaviours in dynamic systems. We did the OPCDs oscillations by integrating a pseudo-Ornstein-Uhlembeck process with mean reversion ($p-OU$). In this way, the integration of an $p-OU$ in an ANFIS model for the identification allows for a set of a Stochastic Flexible ANFIS structure (SF-ANFIS), endowing the model with the ability to identify online stochastic behaviours or disturbances in dynamic systems, which make it ideal for the control of systems that present oscillatory behaviours. The lower persistence of disturbances shows the stability of the SF-ANFIS model in controlling the RFJs in OPCDs with oscillatory behaviours. This stability was promoted by the mean reversion that exhibits the $p-OU$ and the integration of the EDA algorithm, which improves the online learning process. In this way, the convergence of the EDA algorithm was conducted by the $p-OU$, which tends

to bring the systems to the average close to the set point in a better way, unlike the models used to assess the proposed model, which reached the set point for each joint, but a more remarkable persistence of disturbances near to OPCDs. This fact confirms the system's global stability agrees with Lyapunov's theorem for an SF-ANFIS model with a $p - OU$ structure.

According to the fuzzy model proposed by [56], the statistical metrics show that models used to assess the proposed model exhibited in general good behaviours; however, these models reached the set point differently due to the purely linear structure of the MADALINE model that does not allow to identify stochastic behaviours, or the fuzzy neural model proposed by [39], where the sampling method does not have a specific structure to be synchronised with the disturbances or the stochastic behaviour with mean reversion that presents the flexible joints.

In general, the SF-ANFIS- EDA model achieved to overcome the limitations imposed by the directional friction near-maximum negative angles when the signal control takes the maximum values, which makes the model ideal for improving the operational accuracy in this type of RFJs system when it requires stability in the manipulation of highs and dynamical loads.

As future work, we propose using different stochastic models to drive the sampling process in EDA algorithms, according to other complex stochastic behaviours as presented in RFJs, to drive toward a stochastic optimisation to reduce the persistence of persistence disturbances in terms of their behaviour.

7. Annex 1

The Lagrangian equations modeling the main dynamics are shown in Eq. (42)

$$\begin{aligned} L &= \frac{1}{2}\left[m_1 l_{c_1}^2 + m_2 l_1^2\right]\dot{q}_1^2 + \frac{1}{2} m_2 l_{c_2}^2 \left[\dot{q}_1 + \dot{q}_2\right]^2 + \\ &\quad + m_2 l_1 l_{c_2} \cos\left(q_2\right)\left[\dot{q}_1^2 + \dot{q}_1\dot{q}_2\right] + \left[m_1 l_{c_1} + m_2 l_1\right] g \cos\left(q_1\right) + \\ &\quad + m_2 g l_{c_2} \cos\left(q_1 + q_2\right) + \frac{1}{2} I_1 \dot{q}_1^2 + \frac{1}{2} I_2 \left[\dot{q}_1 + \dot{q}_2\right]^2, \end{aligned} \tag{42}$$

where L is the Lagrangian; g is the gravitational constant; m_1, m_2 are the mass of the joints (kg); l_{c_1}, l_{c_2} are the centre of mass for each joint (m); l_1, l_2 are the length for each joint (m); $q_1, q_2 \in \left[-\frac{\pi}{4}, \frac{\pi}{4}\right]$ are the angles for each

joint (rad), and $\dot{q}_1, \dot{q}_2$ their angular velocities; and I_1, I_2 are the momentum for each of the bars ($kg.m^2$).

The oscillatory dynamics can be described according to Euler Lagrange equations as in Eq. (43), (44) and (45)

$$T = \frac{1}{2} m_l l_l^2 \dot{q}_l^2 + \frac{1}{2} I_l \dot{q}_l^2 = \frac{2}{3} m_l l_l^2 \dot{q}_l^2, \tag{43}$$

$$U = mg\left[l_l - l_l \sin\left(q_l\right)\right] + \frac{1}{2} k_{1,l} \left[2R_1 \sin\left(q_l\right)\right]^2 + \frac{1}{2} k_{2,l} \left[R_1 - 2R_2 \sin\left(q_l\right)\right]^2, \tag{44}$$

$$\ddot{q}_l = \frac{3}{4} g \cos\left(q_l\right) - \frac{3R_1 k_{1,l}}{2ml_l} \sin\left(q_l\right) \cos\left(q_l\right) + \frac{3}{2} \left[R_1 - 2R_2 \sin\left(q_l\right)\right] \cos\left(q_l\right) + f_{1f} \dot{q}_l, \tag{45}$$

where T is the kinetic energy; U is the potential energy; $k_{1,l}$, $k_{2,l}$ are the spring constants; l_1, l_2 represent the joints; q_1, q_2: represent the angles of oscillation in OPCDs; and R_1, R_2 represent the radius of the springs in each joint.

8. Annex 2

The parameters, variables and values that define the dynamics of the systems are shown in Table 8.

Table 8: Parameters of the system dynamics

Parameter	Notation	Value	Units
joint length 1	l_1	0.45	m
joint length 2	l_2	0.45	m
link mass 1	m_1	23.902	Kg
link mass 2	m_2	3.880	Kg
link mass center 1	lc_1	0.091	m
link mass center 2	lc_2	0.048	m
moment of inertia 1	I_1	1.266	$Kg.m^2$
moment of inertia 2	I_2	0.093	$Kg.m^2$
viscosity coefficient 1	b_1	2.288	$Nm - seg$
viscosity coefficient 2	b_2	0.175	$Nm - seg$
Coulomb coefficient 1	fc_1	$if\ (q1_{>}0; 7..17)$ $if\ (q_1 < 0; 8.049)$	Nm
Coulomb coefficient 2	fc_2	1.734	Nm
Gravity	g	9.81	$\frac{m}{s^2}$
Torque joint 1	τ_1	150	Nm
Torque joint 2	τ_2	15	Nm
Radius joint 1	R_1	0.15	m
Radius joint 2	R_2	0.15	m
Spring constants - Joint 1	k_{11} k_{21}	1	$\frac{N}{m}$
Spring constants - Joint 2	k_{12} k_{22}	2	$\frac{N}{m}$

Acknowledgments

The authors thank to The EIA University (CO12021002) for the support of the research project that resulted in this article within the framework of the IAPP with the RAE. Likewise, the authors thank the Research Group on Finance and Sustainability from the Universidad Nacional de Colombia for its active support in the environmental and financial sustainability topics. Also, the authors would like to thank the editorial team and anonymous reviewers who contributed to improving this paper's quality.

References

[1] J. Huddy, M. Crockett, A. Nizar, R. Smith, M. Malki, N. Barber, H. Tilney, Experiences of a "covid protected" robotic surgical centre for colorectal and urological cancer in the covid-19 pandemic, Journal of Robotic Surgery 16 (1) (2022) 59 – 64. doi:10.1007/s11701-021-01199-3.

[2] F. Holsinger, A. Birkeland, M. Topf, Precision head and neck surgery: robotics and surgical vision technology, Current opinion in otolaryngology & head and neck surgery 29 (2) (2021) 161 – 167. doi:10.1097/MOO.0000000000000706.

[3] J. Estevez, M. Graña, J. M. Lopez-Guede, Online fuzzy modulated adaptive pd control for cooperative aerial transportation of deformable linear objects, Integrated Computer-Aided Engineering 24 (1) (2017) 41–55. doi:10.3233/ICA-160530.

[4] Y. Matsuda, Y. Sato, T. Sugi, S. Goto, N. Egashira, Control system for object transportation by a mobile robot with manipulator combined with manual operation and autonomous control, International Journal of Innovative Computing, Information and Control 18 (2) (2022) 621 – 631. doi:10.24507/ijicic.18.02.621.

[5] A. Prieto, A. Romero, F. Bellas, R. Salgado, R. J. Duro, Introducing separable utility regions in a motivational engine for cognitive developmental robotics, Integrated Computer-Aided Engineering 26 (1) (2019) 3–20. doi:10.3233/ICA-180578.

[6] E. S. Cross, R. Ramsey, Mind meets machine: Towards a cognitive science of human–machine interactions, Trends in Cognitive Sciences 25 (3) (2021) 200–212. doi:https://doi.org/10.1016/j.tics.2020.11.009.

[7] L. Sabri, S. Bouznad, S. Rama Fiorini, A. Chibani, E. Prestes, Y. Amirat, An integrated semantic framework for designing context-aware internet of robotic things systems, Integrated Computer-Aided Engineering 25 (2) (2018) 137–156. doi:10.3233/ICA-170559.

[8] F. Gomez-Donoso, F. Escalona, F. M. Rivas, J. M. Cañas, M. Cazorla, Enhancing the ambient assisted living capabilities with a mobile robot, Computational Intelligence and Neuroscience 2019 (15) (2019). doi:https://doi.org/10.1155/2019/9412384.

[9] Ozgoli, H. Taghirad, A survey on the control of flexible joint robots, Asian Journal of Control 8 (4) (2006) 332–344. doi:10.1111/j.1934-6093.2006.tb00285.x.

[10] Makris, Tsarouchi, Matthaiakis, Athanasatos, Chatzigeorgiou, Stefos, Giavridis, Aivaliotis, Dual arm robot in cooperation with humans for flexible assembly, CIRP Annals 66 (1) (2017) 13 – 16. doi:https://doi.org/10.1016/j.cirp.2017.04.097.

[11] M. Almagro, V. Fresno, F. de la Paz, Speech gestural interpretation by applying word representations in robotics, Integrated Computer-Aided Engineering 26 (1) (2019) 97–109. doi:10.3233/ICA-180585.

[12] F. J. Rodriguez Lera, F. M. Rico, V. M. Olivera, Neural networks for recognizing human activities in home-like environments, Integrated Computer-Aided Engineering 26 (1) (2019) 37–47. doi:10.3233/ICA-180587.

[13] G. Widmann, S. Ahmad, Control of industrial robots with flexible joints, in: Proceedings. 1987 IEEE International Conference on Robotics and Automation, Vol. 4, 1987, pp. 1561–1566. doi:10.1109/ROBOT.1987.1087789.

[14] G. Iacca, F. Caraffini, F. Neri, E. Mininno, Robot base disturbance optimization with compact differential evolution light, in: Applications of Evolutionary Computation, Springer Berlin Heidelberg, Berlin, Heidelberg, 2012, pp. 285–294.

[15] G. Iacca, F. Caraffini, F. Neri, Multi-strategy coevolving aging particle optimization, International Journal of Neural Systems 24 (01) (2014) 1450008, pMID: 24344695. doi:10.1142/S0129065714500087.

[16] V. T. Yen, W. Y. Nan, P. Van Cuong, Recurrent fuzzy wavelet neural networks based on robust adaptive sliding mode control for industrial robot manipulators, Neural Computing and Applications 31 (11) (2019) 6945–6958. doi:10.1007/s00521-018-3520-3.

[17] P. Khosla, Categorization of parameters in the dynamic robot model, IEEE Transactions on Robotics and Automation 5 (3) (1989) 261 – 268.

[18] J. Wu, J. Wang, Z. You, An overview of dynamic parameter identification of robots, Robotics and Computer-Integrated Manufacturing 26 (5) (2010) 414 – 419. doi:https://doi.org/10.1016/j.rcim.2010.03.013.

[19] Z. Jiang, K. Shinohara, Workspace trajectory tracking control of flexible joint robots based on backstepping method, in: 2016 IEEE Region 10 Conference - TENCON, 2016, pp. 3473–3476. doi:10.1109/TENCON.2016.7848700.

[20] A. M. Kabir, J. D. Langsfeld, K. N. Kaipa, S. K. Gupta, Identifying optimal trajectory parameters in robotic finishing operations using minimum number of physical experiments, Integrated Computer-Aided Engineering 25 (2) (2018) 111–135. doi:10.3233/ICA-180563.

[21] G. Iacca, F. Carafinni, F. Neri, Multi-strategy coevolving aging particle optimization, International Journal of Neural Systems 24 (01) (2014) 1450008. doi:10.1142/S0129065714500087.

[22] G. Iacca, F. Caraffini, F. Neri, E. Mininno, Robot base disturbance optimization with compact differential evolution light, in: D. C. C. et al. (Ed.), Applications of Evolutionary Computation. EvoApplications 2012. Lecture Notes in Computer Science, vol 7248., Springer, Berlin, Heidelberg, 2012, pp. 285–294. doi:10.1007/978-3-642-29178-4_29.

[23] G. Iacca, F. Caraffini, F. Neri, Compact differential evolution light: high performance despite limited memory requirement and modest computational overhead, Journal of Computer Science and Technology 27 (5) (2012) 1056–1076.

[24] G. Iacca, F. Caraffini, F. Neri, Memory-saving memetic computing for path-following mobile robots, Applied Soft Computing 13 (4) (2013) 2003 – 2016.

[25] X. Han, W.-F. Xie, Z. Fu, W. Luo, Nonlinear systems identification using dynamic multi-time scale neural networks, Neurocomputing 74 (17) (2011) 3428 – 3439. doi:https://doi.org/10.1016/j.neucom.2011.06.007.

[26] S. Ilya, V. Oriol, L. V., Sequence to sequence learning with neural networks, in: Proceedings of the 27th International Conference on Neural Information Processing Systems - Volume 2, NIPS'14, MIT Press, Cambridge, MA, USA, 2014, pp. 3104–3112.

[27] J. Tanevski, L. Todorovski, S. Deroski, Learning stochastic process based models of dynamical systems from knowledge and data, BMC Systems Biology 10 (1) (2016) 30. doi:10.1186/s12918-016-0273-4.

[28] J. Hernandez, J. Ospina, A multi dynamics algorithm for global optimization, Mathematical and Computer Modelling 52 (7) (2010) 1271 – 1278, mathematical Models in Medicine, Business & Engineering 2009. doi:https://doi.org/10.1016/j.mcm.2010.03.024.

[29] I. Valdez, A. Hernandez, S. Botello, A boltzmann based estimation of distribution algorithm, Information Sciences 236 (2013) 126 – 137. doi:https://doi.org/10.1016/j.ins.2013.02.040.

[30] S. Mahapatra, R. Daniel, D. N. Dey, S. K. Nayak, Induction motor control using pso-anfis, Procedia Computer Science 48 (2015) 753 – 768, international Conference on Computer, Communication and Convergence (ICCC 2015). doi:https://doi.org/10.1016/j.procs.2015.04.212.

[31] M. Nobile, P. Cazzaniga, D. Besozzi, R. Colombo, G. Mauri, G. Pasi, Fuzzy self-tuning pso: A settings-free algorithm for global optimization, Swarm and Evolutionary Computation (2017). doi:https://doi.org/10.1016/j.swevo.2017.09.001.

[32] H. Lal, S. Sarkar, S. Gupta, Stochastic model order reduction in randomly parametered linear dynamical systems, Applied Mathematical Modelling 51 (2017) 744 – 763. doi:10.1016/j.apm.2017.07.043.

[33] K. Prasad, A. K. Gorai, P. Goyal, Development of anfis models for air quality forecasting and input optimization for reducing the computational cost and time, Atmospheric Environment 128 (2016) 246 – 262. doi:https://doi.org/10.1016/j.atmosenv.2016.01.007.

[34] H. Verdejo, A. Awerkin, E. Saavedra, W. Kliemann, L. Vargas, Stochastic modeling to represent wind power generation and demand in electric power system based on real data, Applied Energy 173 (2016) 283 – 295. doi:https://doi.org/10.1016/j.apenergy.2016.04.004.

[35] Y. Zhang, T. Chai, H. Wang, A nonlinear control method based on anfis and multiple models for a class of siso nonlinear systems and its application, IEEE Transactions on Neural Networks 22 (11) (2011) 1783–1795. doi:10.1109/TNN.2011.2166561.

[36] H. Wang, X. Liu, K. Liu, H. R. Karimi, Approximation-based adaptive fuzzy tracking control for a class of nonstrict-feedback stochastic nonlinear time-delay systems, IEEE Transactions on Fuzzy Systems 23 (5) (2015) 1746–1760. doi:10.1109/TFUZZ.2014.2375917.

[37] C.-Y. Chen, W.-H. Gui, Z.-H. Guan, R.-L. Wang, S.-W. Zhou, Adaptive neural control for a class of stochastic nonlinear systems with unknown parameters, unknown nonlinear functions and stochastic disturbances, Neurocomputing 226 (2017) 101 – 108. doi:https://doi.org/10.1016/j.neucom.2016.11.042.

[38] A. Iolov, S. Ditlevsen, A. Longtin, Stochastic optimal control of single neuron spike trains, Journal of Neural Engineering 11 (4) (2014) 046004.

[39] Jiang, Mahadevan, Yuan, Fuzzy stochastic neural network model for structural system identification, Mechanical Systems and Signal Processing 82 (2017) 394–411. doi:10.1016/j.ymssp.2016.05.030.

[40] D. Wang, D. Liu, Y. Zhang, H. Li, Neural network robust tracking control with adaptive critic framework for uncertain nonlinear systems, Neural Networks 97 (2018) 11 – 18. doi:https://doi.org/10.1016/j.neunet.2017.09.005.

[41] C. Lin, T. Le, T. Huynh, Self-evolving function-link interval type 2 fuzzy neural network for nonlinear system identification and control, Neurocomputing 275 (2018) 2239 – 2250. doi:https://doi.org/10.1016/j.neucom.2017.11.009.

[42] Y. Li, L. Liu, G. Feng, Robust adaptive output feedback control to a class of non-triangular stochastic nonlinear systems, Automatica 89 (2018) 325 – 332. doi:https://doi.org/10.1016/j.automatica.2017.12.020.

[43] X. Xing, Y. Pan, Q. Lu, H. Cui, New mean square exponential stability condition of stochastic fuzzy neural networks, Neurocomputing 156 (2015) 129 – 133. doi:https://doi.org/10.1016/j.neucom.2014.12.076.

[44] B. Carolina, L. Daniel, L. Esteban, P. Alejandro, S. Alejandro, Modelling of Dynamic Real Systems through the Integration of Stochastic Process at the Euler Lagrange Equations, Pascual Bravo Instituion Technologies, 2014.

[45] P. Isazi, I. Galvan, Redes de neuronas artificiales: un enfoque practico, Pearson Educacion, 2004.

[46] Y. Ashida, S. Wakitani, T. Yamamoto, Design of an implicit self tuning pid controller based on the generalized output, IFAC PapersOnLine 50 (1) (2017) 13946 – 13951, 20th IFAC World Congress. doi:https://doi.org/10.1016/j.ifacol.2017.08.2216.

[47] M. Kandroodi, M. Mansouri, M. Shoorehdeli, M. Teshnehlab, Control of flexible joint manipulator via reduced rule-based fuzzy control with experimental validation, ISRN Artificial Intelligence (2012).

[48] C. Zuluaga-Bedoya, J. Garcia-Tirado, S. Gomez, V. H. Jaramillo, Phenomenological based semi-physical model for a pressure control plant, in: 2017 IEEE 3rd Colombian Conference on Automatic Control (CCAC), 2017, pp. 1–6. doi:10.1109/CCAC.2017.8276444.

[49] C. Mitsantisuk, M. Nandayapa, K. Ohishi, S. Katsura, Parameter estimation of flexible robot using multi-encoder based on disturbance observer, in: IECON 2012 - 38th Annual Conference on IEEE Industrial Electronics Society, 2012, pp. 4424–4429. doi:10.1109/IECON.2012.6389473.

[50] A. Calanca, L. M. Capisani, A. Ferrara, L. Magnani, Mimo closed loop identification of an industrial robot, IEEE Transactions on Control Systems Technology 19 (5) (2011) 1214–1224. doi:10.1109/TCST.2010.2077294.

[51] W. Wu, S. Zhu, X. Wang, H. Liu, Closed-loop dynamic parameter identification of robot manipulators using modified fourier series, International Journal of Advanced Robotic Systems 9 (1) (2012) 29. doi:10.5772/45818.

[52] N. J, W. H, A direct adaptive neural network control for unknown nonlinear systems and its application, in: American Control Conference, Proceedings of the 1995, Vol. 6, 1995, pp. 4285–4289 vol.6. doi:10.1109/ACC.1995.532743.

[53] M.-C. Roger, M.-V. Javier, Experimental parameter identification of flexible joint robot manipulators, Robotica 36 (3) (2018) 313–332. doi:10.1017/S0263574717000224.

[54] S. Ulrich, J. Z. Sasiadek, Methods of trajectory tracking for flexible joint space manipulators, IFAC Proceedings Volumes 44 (1) (2011) 10307 – 10312, 18th IFAC World Congress. doi:https://doi.org/10.3182/20110828-6-IT-1002.02189.

[55] B. Subudhi, S. Pradhan, Direct adaptive control of a flexible robot using reinforcement learning, in: 2010 International Conference on Industrial Electronics, Control and Robotics, 2010, pp. 129–136. doi:10.1109/IECR.2010.5720144.

[56] O.-H. Park, M.-G. Seok, Selection of an appropriate model to predict plume dispersion in coastal areas, Atmospheric Environment 41 (29) (2007) 6095 – 6101. doi:https://doi.org/10.1016/j.atmosenv.2007.04.010.

[57] M. David, G. Esther, T. Felipe, R. F., Sintonizador fuera de linea de un controlador pid discreto usando un algoritmo genetico multiobjetivo., Research in Computing Science 113 (2016) 171–180.

[58] R. Sakthivel, T. Saravanakumar, B. Kaviarasan, S. M. Anthoni, Dissipativity based repetitive control for switched stochastic dynamical systems, Applied Mathematics and Computation 291 (2016) 340 – 353. doi:https://doi.org/10.1016/j.amc.2016.07.019.

[59] A. Pena, I. Bonet, C. Lochmueller, A. Patino, F. Chiclana, M. Gongora, A fuzzy credibility model to estimate the operational value at risk using internal and external data of risk events, Knowledge-Based Systems 159 (2018) 98 – 109. doi:https://doi.org/10.1016/j.knosys.2018.06.007.

[60] D. Guleryuz, Forecasting outbreak of covid-19 in turkey; comparison of box–jenkins, brown's exponential smoothing and long short-term memory models, Process Safety and Environmental Protection 149 (2021) 927–935. doi:https://doi.org/10.1016/j.psep.2021.03.032.

[61] R. H. Hirpara, S. N. Sharma, An ornstein-uhlenbeck process-driven power system dynamics, IFAC-PapersOnLine 48 (30) (2015) 409 – 414, 9th IFAC Symposium on Control of Power and Energy Systems CPES 2015. doi:https://doi.org/10.1016/j.ifacol.2015.12.413.

[62] A. Pena, J. Hernandez, V. Toro, Computational evolutionary inverse lagrangian puff model, Environmental Modelling & Software 25 (12) (2010) 1890 – 1893. doi:https://doi.org/10.1016/j.envsoft.2010.04.013.

[63] S. Barak, S. Sadegh, Forecasting energy consumption using ensemble arima–anfis hybrid algorithm, International Journal of Electrical Power & Energy Systems 82 (2016) 92 – 104. doi:https://doi.org/10.1016/j.ijepes.2016.03.012.

Highlights

An Evolutionary Intelligent Control System For A Flexible Joints Robot

Alejandro Pena, Juan C. Tejada, Juan David Gonzalez-Ruiz, Lina María Sepúlveda-Cano, Francisco Chiclana, Fabio Caraffini, Mario A. Gongora

- We present a novel adaptive, flexible stochastic model SF-ANFIS for online control of coupled systems with stochastic behaviours, as shown in RFJs.
- We achieved the theoretical modelling of the RFJs by integrating the Euler Lagrange of two sinusoidal delay signals to model the persistence of the disturbances in OPCDs, setting a novel methodology to model stochastic behaviours in dynamic systems.
- The lower persistence of disturbances shows the stability of the SF-ANFIS model in controlling the RFJs in OPCDs with oscillatory behaviours.
- The SF-ANFIS- EDA model achieved to overcome the limitations imposed by the directional friction near-maximum negative angles when the signal control takes the maximum values, which makes the model ideal for improving the operational accuracy in this type of RFJs system when it requires stability in the manipulation of highs and dynamical loads.

Alejandro Peña P. (PhD)
Information & Management Research Group
Business School
EAFIT University
Carrera 49, Calle 7 Sur #50
Medellín, Colombia (Postal Code: 055022)
Visiting Researcher
Institute for Artificial Intelligence (IAI)
DeMontfort University
Leicester, England
E: japena@eafit.edu.co

December 26, 2022

Re: Credit Author Statement - ASOC-D-22-04393 - *An Evolutionary Intelligent Control System For A Flexible Joints Robot*

Dear Editor-in-Chief,

In the paper the authors' contribution was as follows:

- Alejandro Peña: Conceptualization, Software, Writing Original Draft & Investigation
- Juan C. Tejada: Formal Analysis & Proof of Equations
- Juan David Gonzalez-Ruiz: Formal Analysis & Investigation
- Lina María Sepulveda: Conceptualization, Resources & Analysis
- Francisco Chiclana: Conceptualization, Writing Original Draft, Proof Equations & Analysis.
- Fabio Caraffini: Conceptualization, Writing Original Draft & Proof Equations
- Mario Góngora: Supervision & Project Administrations.

Sincerely yours,

Prof. Alejandro Peña, on behalf of co-authors - Juan C. Tejada, Juan David González-Ruiz, Lina María Sepúlveda-Cano, Francisco Chiclana, Fabio Caraffini, Mario A. Góngora

Declaration of interests

☒ The authors declare that they have no known competing financial interests or personal relationships that could have appeared to influence the work reported in this paper.

☐ The authors declare the following financial interests/personal relationships which may be considered as potential competing interests: